J. Fluid Mech. (1999), *vol.* 390, *pp.* 1–23. Printed in the United Kingdom

An experimental insight into the effect of confinement on tip vortex cavitation of an elliptical hydrofoil

By OLIVIER BOULON, MATHIEU CALLENAERE, JEAN-PIERRE FRANC AND JEAN-MARIE MICHEL

Laboratoire des Ecoulements Géophysiques et Industriels – Institut de Mécanique de Grenoble, BP 53-38041, Grenoble Cedex 9, France

(Received 7 July 1997 and in revised form 28 May 1998)

The present paper is devoted to an analysis of tip vortex cavitation under confined situations. The tip vortex is generated by a three-dimensional foil of elliptical planform, and the confinement is achieved by flat plates set perpendicular to the span, at an adjustable distance from the tip. In the range of variation of the boundary-layer thickness investigated, no significant interaction was observed between the tip vortex and the boundary layer which develops on the confinement plate. In particular, the cavitation inception index for tip vortex cavitation does not depend significantly upon the length of the plate upstream of the foil. On the contrary, tip clearance has a strong influence on the non-cavitating structure of the tip vortex and consequently on the inception of cavitation in its core. The tangential velocity profiles measured by a laser-Doppler velocimetry (LDV) technique through the vortex, between the suction and the pressure sides of the foil, are strongly asymmetric near the tip. They become more and more symmetric downstream and the confinement speeds up the symmetrization process. When the tip clearance is reduced to a few millimetres, the two extrema of the velocity profiles increase. This increase results in a decrease of the minimum pressure in the vortex centre and accounts for the smaller resistance to cavitation observed when tip clearance is reduced. For smaller values of tip clearance, a reduction of tip clearance induces on the contrary a significant reduction in the maxima of the tangential velocity together with a significant increase in the size of the vortex core estimated along the confinement plate. Hence, the resistance to cavitation is much higher for such small values of tip clearance and in practice, no tip vortex cavitation is observed for tip clearances below 1.5 mm. The cavitation number for the inception of tip vortex cavitation does not correlate satisfactorily with the lift coefficient, contrary to classical results obtained without any confinement. Owing to the specificity introduced by the confinement, the usual procedure developed in an infinite medium to estimate the vortex strength from LDV measurements is not applicable here. Hence, a new quantity homogeneous to a circulation had to be defined on the basis of the maximum tangential velocity and the core size, which proved to be better correlated to the cavitation inception data.

1. Introduction

The prediction of tip vortex cavitation inception is a complex problem which has been approached by many investigators and which is of practical interest for marine propellers. In general, the inception cavitation number σ_i is supposed to be given

by the minimum value of the pressure coefficient $-C_{p,min}$ (Knapp, Daily & Hammitt 1970). In the case of attached cavitation on a foil, it is well known that this basic law may be significantly altered by viscous and turbulent effects and by the water quality. In the case of the trailing vortex which develops at the tip of a finite span hydrofoil, it is still a challenge to predict where the minimum pressure will occur along the vortex path and what its value will be. Moreover, as in the case of attached cavitation, the conditions of inception in the vortex core are sensitive to other parameters such as turbulence and water quality. Concerning the water quality, i.e. nuclei and dissolved gas content its influence on tip vortex cavitation was proved by several experimenters (Arndt, Arakeri & Higuchi 1991; Arndt & Keller 1991; Gowing *et al.* 1995; Briançon-Marjollet & Merle 1996). It was confirmed, in the case of an oscillating hydrofoil, by Boulon, Franc & Michel (1997) who showed that the time necessary for a nuclei to be captured by the vortex can strongly delay cavitation inception in the tip vortex. As for the effect of turbulence, Arndt *et al.* (1991) reached the conclusion that no complete correlation is possible without knowledge of the fluctuating levels of pressure in the tip vortex flow.

The non-cavitating structure of the tip vortex flow has been investigated by several experimenters from laser-Doppler velocimetry (LDV) measurements of the flow velocity within the vortex. Fruman *et al.* (1992) have shown that the measured tangential velocity profiles can be approached fairly well by classical theoretical profiles, such as that of Lamb, with two adjusted parameters, the vortex strength Γ and its core radius a. These authors proved that the core radius is correlated to the thickness of the boundary layer which develops on the foil, as assumed by McCormick (1962) in its original work. Concerning the vortex strength, the results of Fruman *et al.* (1991, 1992) demonstrate that the roll-up process is well initiated at the tip of the wing where the local vortex strength reaches about 25% of the total circulation around the tested elliptical foil. The roll-up is half-way to completion at the wing trailing edge, half a chord downstream of the tip. Such velocity profiles, measured with a high spatial resolution, have been integrated by Arndt *et al.* (1991) and Fruman *et al.* (1992) to estimate the minimum pressure coefficient $C_{p,min}$ along the vortex path. According to Fruman *et al.* (1992), the minimum of the pressure coefficient occurs at a short distance from the tip, below 0.2 chord. Both authors show that the values of $-C_{p,min}$ are consistent with the incipient cavitation numbers σ_i. This conclusion was confirmed by several experiments aimed at analysing the effects of various parameters on tip vortex cavitation inception, as the effect of cross-section (Pauchet *et al.* 1994) and planform (Fruman *et al.* 1995*a*). The inhibition of cavitation by polymer injection can also be interpreted in terms of changes in the tangential velocity profile. Fruman *et al.* (1995*b*) show that it is due to an increase of the radius of the vortex core without significant changes of the roll-up of the vortex sheet and therefore of the vortex strength. However, Arndt *et al.* (1991) question the validity of such a procedure of integration of the measured tangential velocity profile for estimating the incipient cavitation number, especially in the presence of strong asymmetric profiles and possibly large axial flow velocities. In this framework, the three-dimensional computations of the whole viscous flow field carried out, for instance, by Dupont & Cerrutti (1992) or Deniset (1996) are promising. A reasonable agreement between computed and measured velocity profiles was obtained by Deniset (1996), although further developments are necessary before a quantitative prediction of cavitation inception becomes possible without model tests.

From a practical viewpoint, it is interesting to establish correlations between cavitation inception data and global parameters of the flow. If we assume a good agreement

between the critical cavitation number and the minimum pressure coefficient at the vortex centre, σ_i should vary as Γ^2/a^2. On the one hand, the vortex strength Γ depends directly upon the circulation around the foil, i.e. upon the lift coefficient C_l. On the other hand, the viscous core radius a is correlated to the boundary-layer thickness and should vary as $Re^{-0.2}$ in the case of a turbulent boundary layer. Hence, the critical cavitation number should vary as $C_l^2 Re^{0.4}$. Several research workers have proposed such correlations (McCormick 1962; Billet & Holl 1979; Fruman *et al.* 1992; Maines & Arndt 1993, 1997). Although the above-mentioned trends with Reynolds number and lift coefficient are generally suitable for a given foil, there seems to be no universal correlation regardless, in particular, of the cross-section and the planform of the three-dimensional foil. Maines & Arndt (1997) show, in the case of three hydrofoils of elliptic planform but of different cross-sections presenting a linear relationship between σ_i and $C_l^2 Re^{0.4}$, that the constant of proportionality is different and may be related to the development of the boundary layer and its interaction with the tip vortex. Let us notice that for tests conducted at low Reynolds numbers, below laminar to turbulent transition, it may be necessary to trip the boundary layer by turbulence promoters in order to extrapolate cavitation inception data to higher Reynolds numbers on the basis of the previous correlations (Pichon, Fruman & Billard 1995). As for the influence of the free-stream turbulence intensity, Pauchet, Viot & Fruman (1996) have shown, by using turbulence generators upstream of the test section, that the critical cavitation numbers are only slightly modified, in their range of variation of the turbulence intensity, and that the modifications are essentially correlated with the changes of the lift coefficient.

All the above-mentioned studies are relative to hydrofoils of finite span in a quasi-infinite medium. Significant changes can be expected if the vortex sheet rolls up in the vicinity of a wall, as is the case for shrouded propellers. The present study is precisely an experimental analysis of the effect of confinement on tip vortex cavitation. Related works can be found in the field of turbomachinery. For compressors, several studies have been carried out to predict the nature of the tip clearance flow and the associated losses (e.g. Lakshminarayana & Horlock 1962). In liquid-handling machinery, the tip clearance flow is complicated by the development of cavitation. In axial-flow pumps, two cavitation patterns can occur, tip clearance cavitation and tip vortex cavitation. Tip clearance cavitation is due to the separation of the flow as it passes between the blade end and the casing wall. It can generally be prevented by rounding the clearance edge on the pressure side, as shown by Laborde *et al.* (1995). Tip vortex cavitation develops in the low-pressure region of the vortex core attached to the blade tip. Gearhart & Ross (1991) and Farrell & Billet (1994) have pointed out an optimum tip clearance for cavitation performance: below this optimum value, a reduction in tip clearance leads to an increase in the inception cavitation number; above it, the cavitation inception number asymptotically increases with tip clearance, up to a value which is characteristic of an unshrouded pump. We shall see in § 4 that the case investigated differs significantly from the case of axial-flow pumps; in addition to important differences in geometries and especially in planforms, significant changes can be expected between rotating blades and the case investigated here of a stationary hydrofoil in a hydrodynamic tunnel.

In the present study, the confinement is achieved by a flat plate, set perpendicular to the span direction, at an adjustable distance from the tip. Such a configuration is characterized by two main parameters, the gap between the plate and the foil tip, and the length of the plate upstream of the tip which controls the boundary-layer state (laminar or turbulent) and its thickness. In the present work, the latter parameter

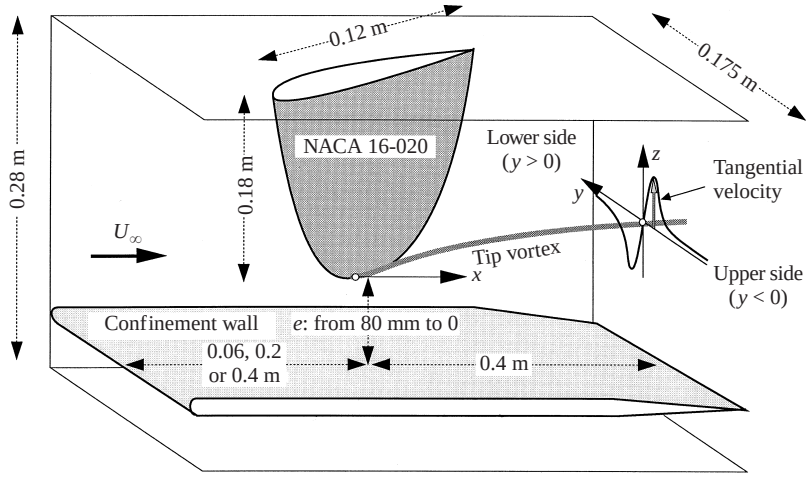

FIGURE 1. Test section and foil arrangement.

appeared to have only a very slight influence on cavitation performance. As explained in § 4, this is due to the contraction of the wake which makes the tip vortex escape from the boundary layer very rapidly. Much longer plates than the ones used in the present study would be required to produce a substantial effect of the boundary layer on tip vortex roll-up and cavitation. Consequently, our main objective was to analyse the effect of a gap reduction on the inception of tip vortex cavitation.

The experimental facility is presented in § 2, together with some general features of the flow. Section 3 is devoted to the presentation of the experimental results, including visualizations and measurements of critical cavitation numbers, which clearly demonstrate the influence of confinement on tip vortex cavitation. These observations are discussed in § 4 on the basis (i) of the measured tangential velocity profiles through the non-cavitating vortex, (ii) of the measured lift coefficient, and (iii) of a simplified potential approach based on the use of an image vortex to take into account the effect of the confinement.

2. Experimental facility and general features of the flow

The tests were conducted in the first test section of the hydrodynamic tunnel of the Institute of Mechanics of Grenoble (Briançon-Marjollet & Michel 1990). The flow velocity U_∞ can be varied between 3 and 12 m s^{-1} and the free-stream turbulence level is about 1.5% without any obstacle in the test section. The Reynolds number based on chord length at root, $c = 0.12$ m, lies between 0.36×10^6 and 1.4×10^6. Most tests were carried out at a flow velocity of 7 m s^{-1} and a Reynolds number of about 0.9×10^6. The dimensions of the test section are 0.28 m $\times$ 0.175 m. It is equipped with a classical hydrodynamic balance, mounted on the wall, which permits measurement of the global lift coefficient from the signal of strain gauges.

The tested hydrofoil has a NACA 16-020 cross-section, an elliptical planform, a relative thickness of 20%, a chord length at root of 0.12 m, a span length of 0.18 m and an aspect ratio A of 3.8. It is mounted vertically in the test section as shown in figure 1. The distance, e, between the foil tip and the horizontal flat plate which confines the flow is adjustable from 0 to 80 mm. The case $e = 60$ mm is generally chosen as the reference case corresponding to no confinement; the increase of lift

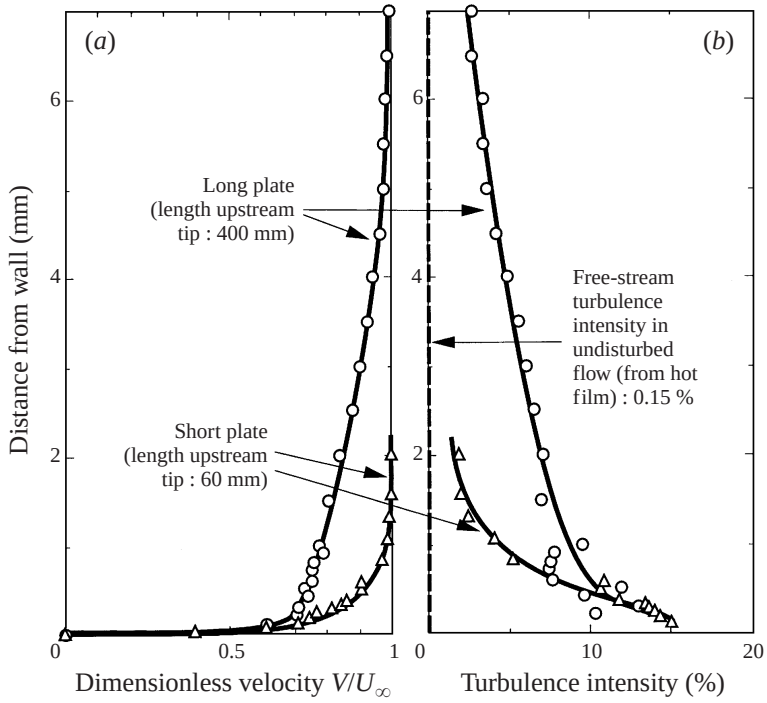

FIGURE 2. (*a*) Velocity and (*b*) turbulence intensity profiles in the boundary layer for the longer and the shorter plates at tip location and for a velocity of $7\,\mathrm{m\,s^{-1}}$. (N.B. The free-stream turbulence intensity is overestimated in comparison with hot-film measurements because of the much higher noise of the laser velocimeter.)

between the case $e \to \infty$ and $e = 60\,\mathrm{mm}$ has been computed to be only 2% (Deniset 1996). The confinement due to the two vertical walls is not negligible; the corresponding increase of lift is 27%, in comparison with the infinite case (Deniset 1996).

Three plates have been designed, corresponding to three different lengths upstream of the foil tip: 0.40 m, 0.20 m and 0.06 m. The velocity and turbulence intensity in the boundary layer were measured by LDV. These measurements were carried out for the larger tip clearance, $e = 80\,\mathrm{mm}$, which minimizes the interaction with the foil. The corresponding profiles at the tip location, where the vortex originates, are given in figure 2. The increase of turbulence intensity in the boundary layer is clear, as well as the increase in boundary-layer thickness when the length of the plate increases.

The plates are 16 mm thick and their nose is elliptical. The side tips of the confinement plates have been rounded and a clearance of 5 mm has been made between the rounded tip and the side walls (see figure 3). This design has been chosen in order to avoid any side cavitation, which could have obstructed the view of the tip vortex. On the other hand, this clearance generates a parasitic flow between the upper and the lower sides of the plate. Figure 3 shows that the central part of the test section, where the tip vortex develops, is unaltered by this secondary clearance flow.

The tangential velocity profiles in the non-cavitating vortex were measured by LDV. The vertical component is determined at various locations along an horizontal axis, y, which goes through the vortex centre (see figure 1). Special care was taken to locate the vortex centre with precision, in order to avoid any bias in the measurements

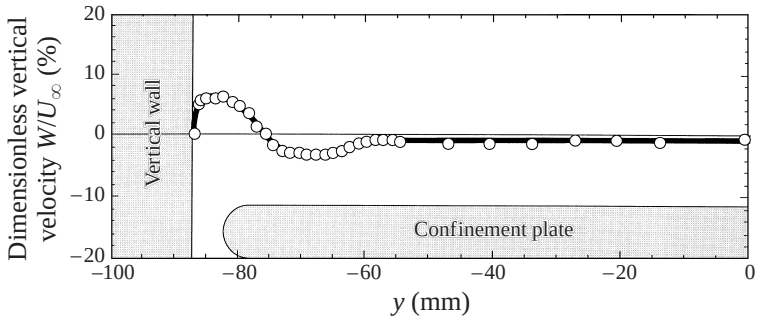

FIGURE 3. Effect of confinement wall on flow field: vertical velocity profile across the test section, at tip height, at 1.25 chord upstream foil tip and for a velocity of $7\,\mathrm{m\,s^{-1}}$ (longer plate).

(Boulon 1996). Although the vortex core is far from being axisymmetric, especially for high degrees of confinement, velocity measurements in the tip vortex have been limited to profiles of the vertical component of the velocity along a horizontal axis going through its centre. A beam expander is used in order to reduce the size of the measuring volume and make the measurement as local as possible inside the vortex core. The intersection of the two laser beams is an ellipsoid of size $0.7\,\mathrm{mm} \times 0.078\,\mathrm{mm}$. The LDV measurements are given with a precision of about $0.05\,\mathrm{m\,s^{-1}}$.

The uncertainties on incipient cavitation numbers and incipient angles of attack are, respectively, of the order of $\pm 0.05^\circ$ and $\pm 0.2^\circ$. These estimates result from various series of tests carried out independently by several experimenters. The uncertainties on the determination of the flow parameters (as velocity and pressure) are negligible in comparison with differences of visual appreciation of cavitation inception or defaults of reproducibility.

3. Experimental results

3.1. *Visualizations*

Visualizations of cavitation in the tip vortex were conducted for various operating conditions of flow velocity, pressure and angle of attack. For each case, the tip clearance, e, is continuously decreased from 60 mm to a few tenths of a millimetre only. Figure 4 gives a typical example of the effect of confinement on tip vortex cavitation.

The cavitation number was chosen so that the reference conditions, assimilated to no confinement (clearance of 60 mm), are non-cavitating (figure 4*a*). For the chosen value of the cavitation parameter, 2.6 in the case of figure 4, no cavitation occurs in the tip vortex as long as tip clearance remains above 20 mm.

For a clearance of about 20 mm, a continuous vapour core suddenly appears. It is stable, but not attached to the tip, as shown in figure 4(*b*). Its head is located at a fixed point $x/c \approx 0.12$, where x is the downstream distance measured from the tip of the foil. This observation may be associated with estimates of the minimum pressure coefficient along the vortex path, as carried out, for example, by Arndt *et al.* (1991), from measured tangential velocity fields. According to Fruman *et al.* (1995*b*), a minimum C_p probably exists between his measurement stations $x/c = 0.125$ and $x/c = 0.25$. Hence, we have to question whether the head of the vapour core observed here does, in fact, correlate with the minimum pressure point along the vortex path.

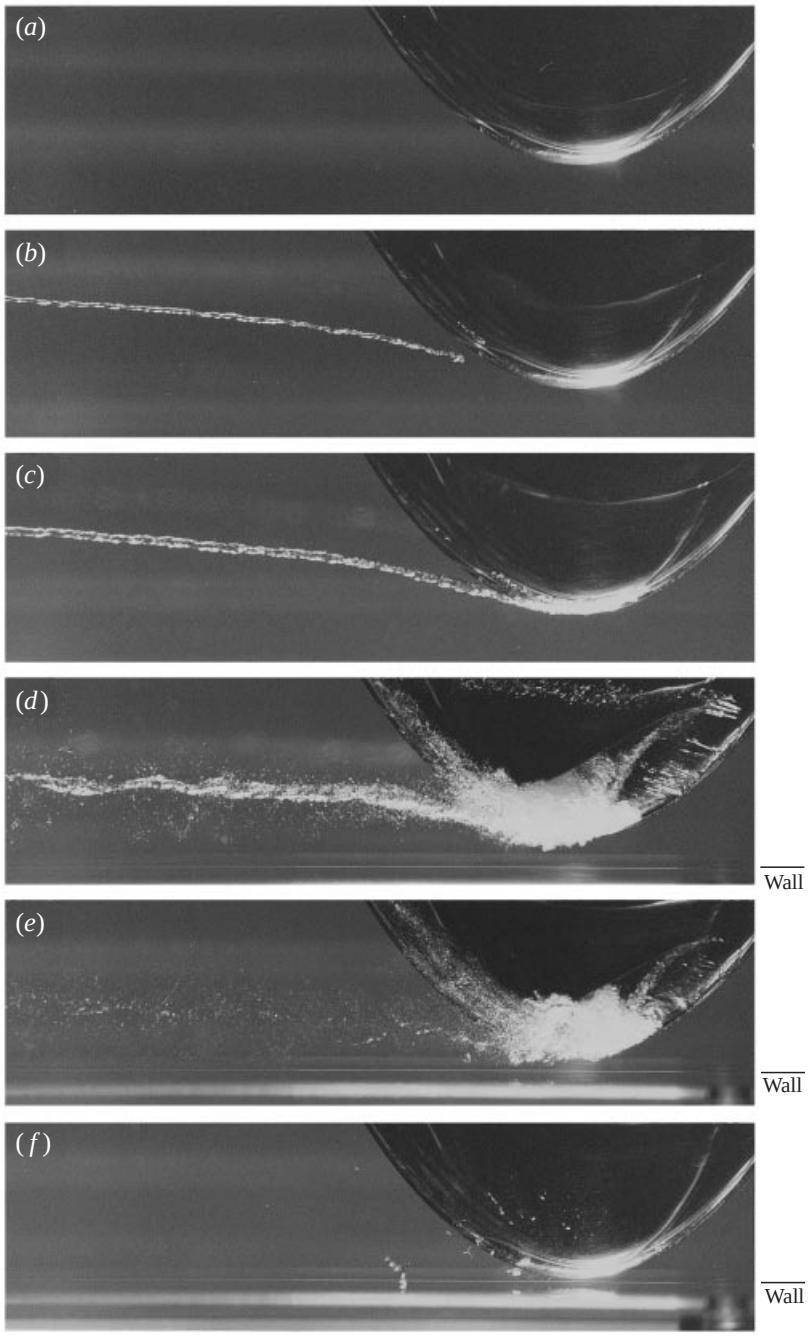

FIGURE 4. Visualizations of tip vortex cavitation for various values of tip clearance (flow velocity 7 m s^{-1}, angle of attack 12°, cavitation number 2.6). (*a*) $e = 50$ mm, (*b*) 20 mm, (*c*) 13 mm, (*d*) 4 mm, (*e*) 2 mm, (*f*) 0.5 mm.

As the tip clearance is further reduced, the vapour core extends towards the foil tip; for $e = 13$ mm (figure 4*c*), it attaches to the tip. It should be pointed out that the critical cavitation conditions considered in the present study, as the inception cavitation number, are the conditions for which the vapour core attaches to the tip. They correspond to a degree of development of cavitation somewhat more advanced than typical cavitation inception defined by the 'first bubble'. The difference $\Delta\sigma$ between the two criteria is of the order of 1 (Boulon *et al.* 1997). The reason for this choice is the very good reproducibility of the conditions of attachment of the vapour core, contrary to the criterion based on the 'first bubble', which is much more dependent upon the experimenter and other parameters, particularly the nuclei content (Boulon *et al.* 1997). In the opinion of the authors, the criterion based on the occurrence of a permanent vapour core attached to the tip gives a good account of inception and limits the subjectivity of measurements for incipient tip vortex cavitation.

For smaller values of the clearance (figure 4*d*), in addition to the tip vortex cavitation, a leading-edge cavity originates in the laminar separation bubble. First, for $13\text{ mm} > e > 6\text{ mm}$, the leading-edge cavity grows towards the foil root. Hence, for $e < 6$ mm, it shrinks towards the tip, when the clearance is decreased. Two different parts are visible on the cavity interface (see for instance figure 4*d*). The part closer to the tip is highly disturbed and wavy, which tends to prove that the flow is turbulent; on the contrary, the part closer to the root is glossy, which gives evidence of a laminar flow above the interface, as demonstrated by other investigations (Franc & Michel 1985). These observations tend to prove that transition to turbulence is not uniform across the wingspan. This point is also valid in non-confined situations as shown by a series of preliminary boundary-layer visualizations by dye injection which demonstrated that the transition to turbulence propagates from tip to root if the angle of attack increases. In the confined case, this phenomenon is emphasized by the effect of induced incidence due to the confinement plate, as the effective angle of attack is higher at the tip than at the root (see § 4.2).

The cavitating vortex is highly disturbed by the development of turbulence. It is barely visible for a clearance of only 2 mm (figure 4*e*). For highly confined flows (figure 4(*f*), $e = 0.5$ mm), leading-edge cavitation, as well as tip vortex cavitation, practically vanish. Cavitation appears in the form of unsteady small cavitating structures, which are a general characteristic of separated flows (Belahadji, Franc & Michel 1995). Hence, the present visualizations tend to prove that the flow is separated in the vicinity of the tip, in highly confined situations. This separated flow pattern is due to the important increase in angle of attack, induced by the mirror image effect of the confinement wall (see § 4.2). The tip vortex does not cavitate for highly confined flows. If the cavitation parameter is further decreased, a leading-edge cavity fills in the separated zone, but no tip vortex is made visible by cavitation. This observation will be discussed on the basis of LDV measurements in § 4.1.

3.2. *Critical cavitation number*

Figure 5 gives the critical cavitation number versus the angle of attack for various values of tip clearance, from the practically non-confined case ($e = 60$ mm) to high confinements ($e = 1.5$ mm). No data are given for smaller values of tip clearance, as no tip vortex cavitation can be observed, as mentioned above. The tests were carried out by progressively reducing the ambient pressure, at a fixed angle of attack. The critical cavitation number corresponds to the limit value for which a continuous vapour core attaches to the foil tip, as explained in § 3. No measurements of desinent cavitation were made although a significant hysteresis was observed especially in confined geometries.

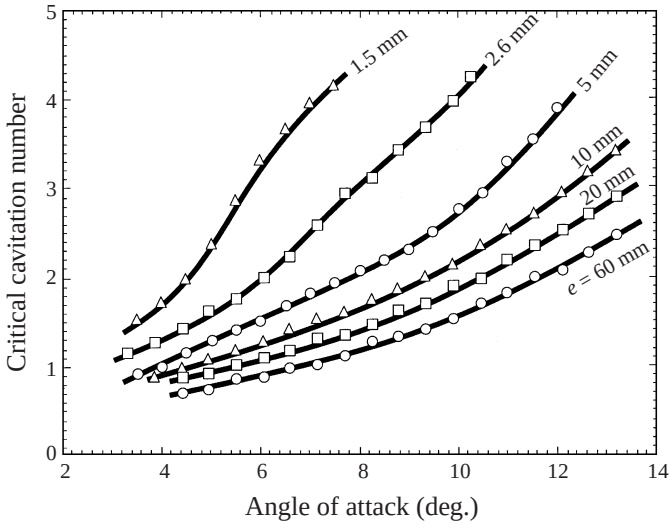

FIGURE 5. Effect of confinement on critical cavitation number versus angle of attack for the long plate, at $7\,\mathrm{m\,s^{-1}}$.

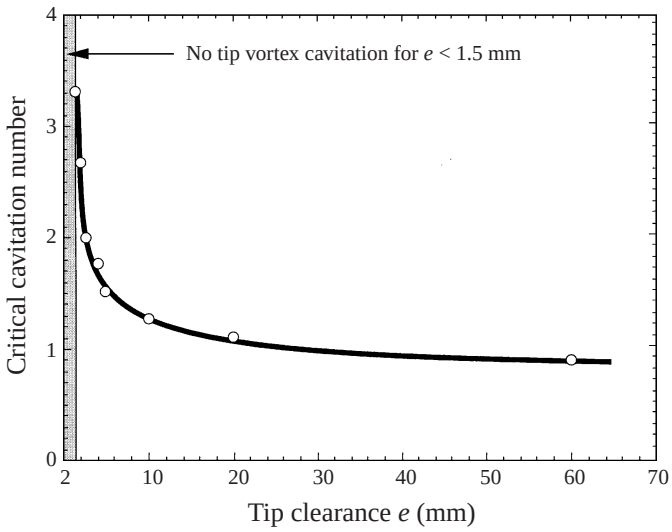

FIGURE 6. Influence of tip clearance on critical cavitation number for an angle of attack of 6° and a flow velocity of $7\,\mathrm{m\,s^{-1}}$.

It can be seen that the confinement induces a large advance in cavitation inception. At an angle of attack of 7° for instance, the critical cavitation number is about 1 for the non-confined flow ($e = 60\,\mathrm{mm}$), whereas it is about 4 in the confined case $e = 1.5\,\mathrm{mm}$. The present trend, shown in figure 6, appears to be different from that obtained by Gearhart & Ross (1991) and Farrell & Billet (1994) on axial flow pumps. These authors show that the inception cavitation number presents a minimum for an optimum value of about 0.2 of the dimensionless tip clearance λ, defined as the ratio of tip clearance to blade thickness at the tip.

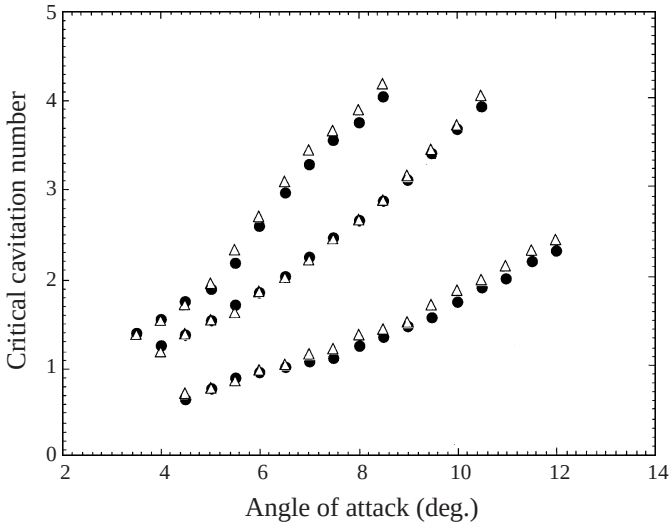

FIGURE 7. Comparison of critical cavitation numbers versus angle of attack for △, the longer (upstream length 400 mm) and ●, the shorter (upstream length 60 mm) confinement plates at flow velocity of $7\,\mathrm{m\,s^{-1}}$.

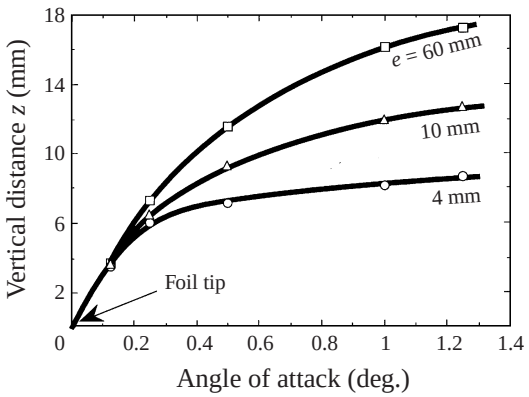

FIGURE 8. Influence of tip clearance on the non-cavitating vortex path for a flow velocity of $7\,\mathrm{m\,s^{-1}}$ and an angle of attack of 8°. (At each station, the vortex centre is determined from LDV measurements.)

Figure 7 presents a comparison of critical cavitation numbers for the longer and the shorter confinement plates. Considering the uncertainties on the determination of the critical cavitation number, we can conclude that the boundary layer which develops on the confinement plate has no significant effect on tip vortex cavitation inception. We could have expected a significant influence if the vortex path were inside the boundary layer. For a clearance of 2 mm, figure 2 shows that, in the boundary layer, the velocity at the tip location is already equal to 85% of the free-stream velocity, for the longer plate. In addition, the contraction of the wake leads the vortex to move away from the confinement plate by about 3.6 mm at 0.125 chord downstream of the tip (see figure 8). Hence, the tip vortex cannot be strongly affected by the boundary layer, even in the case of the longer plate. The confinement effect pointed out in the present work is mainly of a potential nature and is not connected with viscosity.

4. Discussion

4.1. *Cavitation inception and tangential velocity profiles*

The data on cavitation inception are generally interpreted on the basis of the non-cavitating flow. In the case of tip vortex cavitation, the data which are relevant for such a discussion are the tangential velocity profiles across the vortex. The effect of confinement on the profiles of tangential velocity in the non-cavitating tip vortex are given in figure 9 for three different downstream locations. At each location, we compare the profiles obtained for three different values of tip clearance: 4 mm, 10 mm and 60 mm.

Confinement causes an increase in the two extrema of the velocity profile. This effect is more important on the lower side ($y > 0$) than on the upper side ($y < 0$). It induces a decrease in pressure in the vortex core, as we can imagine if we use the classical way of estimating the pressure by integrating the velocity profiles according to Euler's equation (e.g. Arndt *et al.* 1991):

$$\frac{\partial p}{\partial r} = \rho \frac{V^2}{r}. \tag{1}$$

This point is qualitatively consistent with the fact that the critical cavitation number increases when tip clearance is decreased, as shown in figure 6. From a quantitative viewpoint, the prediction of critical cavitation number based on the integration of (1) is not satisfactory, especially in confined situations, as shown by Boulon (1996). It is the reason why those results are not presented here. One of the difficulties is the estimation of the reference pressure from which the integration of (1) is carried out, particularly on the lower side because of the foil wake. The discrepancy may also be due to the increasing lack of axisymmetry with confinement.

If we define the diameter of the vortex core as the distance between the two extrema of flow velocity, it appears, from figure 9, that confinement causes a slight increase in the size of the vortex along the y-axis, parallel to the plate. This observation is consistent with computations (Deniset 1996) which show that the rolled-up vortex sheet, which has a roughly circular shape in an infinite medium, is elongated along the plate and compressed along an axis perpendicular to the plate in confined situations.

The velocity profiles are strongly asymmetric near the tip. They become more and more symmetric as we move downstream. In addition, confinement speeds up the symmetrization process. Let us notice that the undulation observed on the lower side of the velocity profile at station $x/c = 0.125$ is predicted by a purely potential flow computation (Deniset 1996).

To better understand the absence of tip vortex cavitation for very high degrees of confinement (see figures 4(*e*) and 4(*f*)), a series of complementary LDV measurements were conducted for small tip clearances. They show that the structure of the non-cavitating vortex is very different from that at higher tip clearances. Figure 10 shows that, when tip clearance is reduced, the maximum tangential velocity first increases as discussed above, and then strongly decreases. Simultaneously, the size of the vortex core grows very significantly. It is well known that the estimation of the size of the vortex core as well as the estimation of the maximum tangential velocity may be made worse by vortex spatial wandering (see e.g. Straka & Farrell 1992; Fruman *et al.* 1994; Le Guen *et al.* 1997). Then, the problem is to appreciate the possible influence of vortex wandering on the observed evolution of the velocity profiles when tip clearance is reduced.

To clear up this problem, we plot in figure 11 the measured r.m.s. values of the

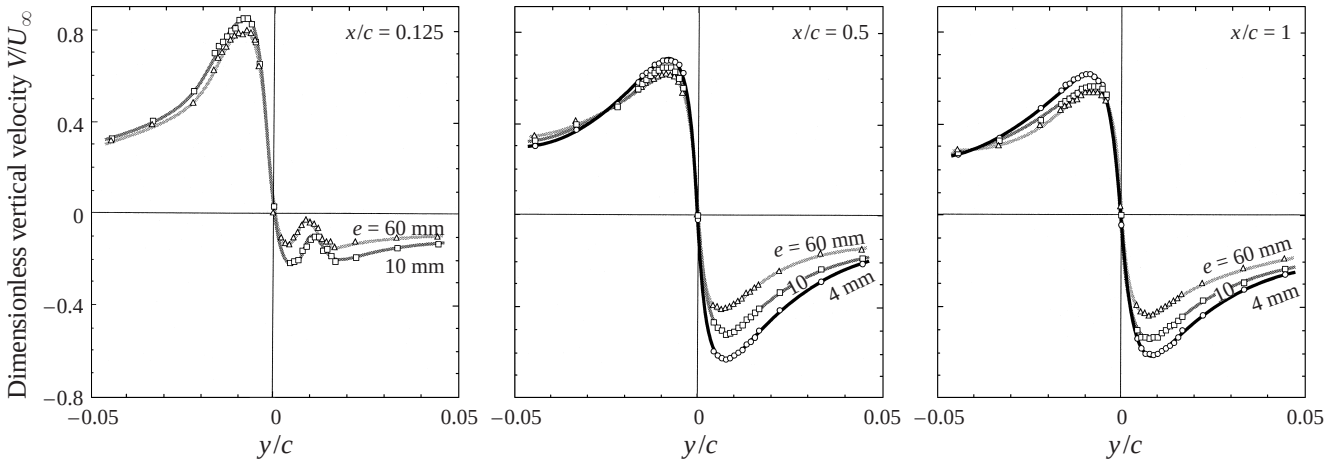

FIGURE 9. Tangential velocity profiles measured by LDV for a flow velocity of $7\,\mathrm{m\,s^{-1}}$ and an angle of attack of 8°. Influence of confinement and of downstream measurement location. (For $x/c = 0.125$ and $e = 4\,\mathrm{mm}$, one of the two laser beams is cut by the confinement plate and the velocity measurement is impossible.)

tangential velocity across the vortex. The r.m.s. distribution corresponding to the less confined case ($e = 60$ mm) exhibits a strong maximum at the vortex centre. This distribution is very similar to those obtained by Arndt & Keller (1991) and Fruman *et al.* (1992) without any confinement. When the tip clearance is reduced, the maximum at the vortex centre decreases greatly, whereas the fluctuations outside the vortex core tend to increase. The large values of the tangential velocity fluctuations in the viscous core for the less confined case are mainly due to vortex wandering. This is qualitatively proved by figure 12.

To build this figure, we considered a normalized vortex of Burgers type and we supposed that its axis can move along a straight line with the amplitude $\pm \frac{1}{2}\Delta r$. With the LDV technique, the measurement is conducted at a fixed point in space, and therefore the vortex wandering results in a measured velocity which corresponds to a mean value estimated over the distance Δr. Figure 12(*a*) presents the influence of the amplitude of vortex wandering Δr on the apparent velocity profile, whereas figure 12(*b*) presents the apparent fluctuations of tangential velocity across the vortex. From those figures, it is clear that an increase in the amplitude of vortex wandering leads to (i) an increase in the apparent size of the viscous core, (ii) a decrease in the maximum tangential velocity, and (iii) an increase in the velocity fluctuations more especially in the vortex core. Note that the finite size of the measuring volume leads to qualitatively similar conclusions. More sophisticated models have been developed, e.g. by Straka & Farrell (1992) and Le Guen *et al.* (1997), but the present simplified model is enough for a qualitative interpretation of the measurements.

Returning to figures 10 and 11, and because of the relatively low fluctuations of tangential velocity in the highly confined configurations, it can be concluded that the vortex excursions are small relative to the size of the core and therefore do not significantly alter the measured tangential velocity profiles for $e = 1.9$ mm and 2.5 mm. On the contrary, in the two cases corresponding to less confined configurations ($e =$ 60 mm and 7 mm), the marked maximum of velocity fluctuations in the vortex centre let us presume that the actual maximum velocity is probably somewhat higher than the measured one and that the size of the viscous core is still smaller, the corrections depending upon the unknown amplitude of vortex wandering. Hence, the observed increase in the size of the viscous core and the observed decrease in the maximum tangential velocity when tip clearance is reduced are not due to vortex wandering but depict an actual modification of the vortex structure. We can imagine that the vortex is compressed by the plate and elongated along it, as already mentioned, which could explain the larger size of its core in the direction of measurement. Moreover, the roll-up of the vortex sheet is more and more restrained by the plate when the tip clearance is decreased, which could explain the decrease in maximum velocity.

The influence of this change in the vortex structure on cavitation inception can easily be inferred. If, for a qualitative discussion, we use the Rankine model to estimate the pressure, the difference between the pressure at infinity and the minimum pressure on the vortex axis is equal to the dynamic pressure ρV_{max}^2, where V_{max} is the maximum velocity. When the tip clearance goes from 7 mm to 1.9 mm, the maximum velocity is divided by about 3, and the minimum pressure coefficient should be divided by about 9. Therefore, for very high confinements, inception cavitation number for tip vortex is very small and, in practice, shear cavitation or leading-edge cavitation develop first.

4.2. *Critical cavitation number and lift*

Most results presented above tend to prove that the effect of confinement is qualitatively equivalent to an increase in angle of attack. This can be understood by

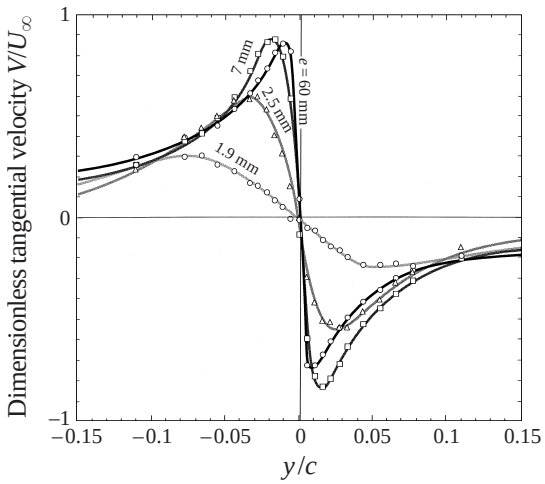

FIGURE 10. Tangential velocity profiles measured by LDV for a flow velocity of $5\,\mathrm{m\,s^{-1}}$, an angle of attack of 12° and at a dimensionless downstream location $x/c = 1$. Influence of tip clearance.

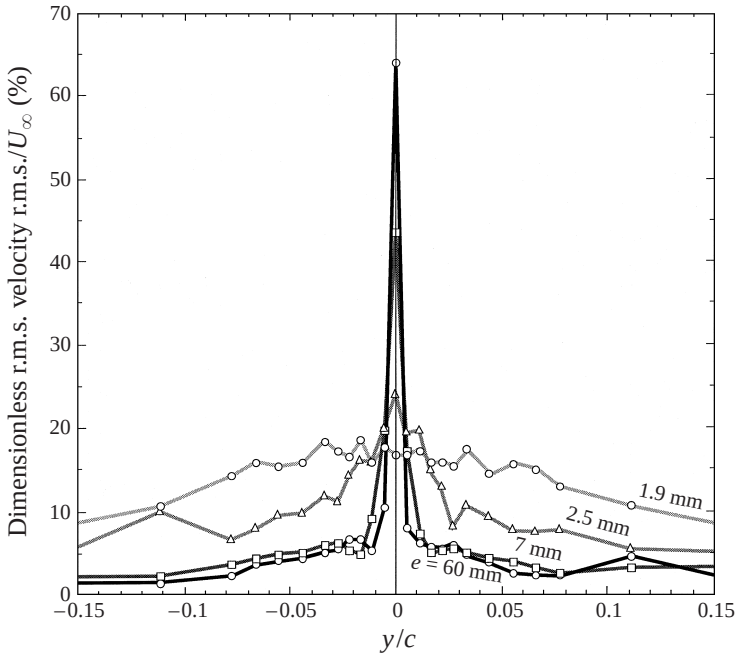

FIGURE 11. Profiles of the r.m.s. values of the tangential velocity for a flow velocity of $5\,\mathrm{m\,s^{-1}}$, an angle of attack of 12° and at a dimensionless downstream location $x/c = 1$. Influence of tip clearance. (The data of figure 11 correspond to the same measurements as figure 10.)

considering the image vortex, symmetrical to the actual tip vortex with respect to the confinement wall. From a purely potential viewpoint, the reason for considering this fictitious vortex is to ensure zero flow across the wall. The image vortex induces a velocity, V_i, shown in figure 13. It has to be combined with the velocity at infinity, U_∞, to obtain the actual attack velocity. From the top view, it is clear that the geometric angle of attack, α, is increased by the induced angle, α_i. The latter is a maximum at the

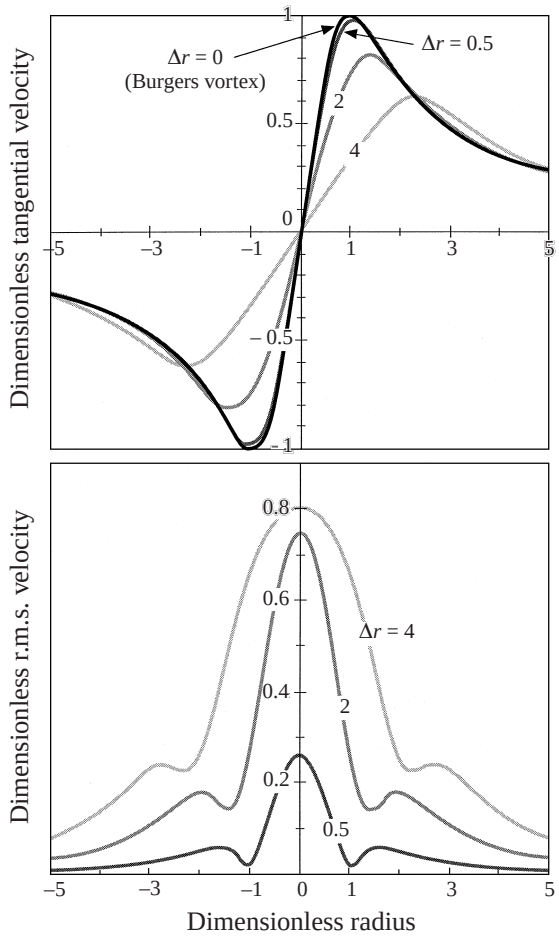

FIGURE 12. Influence of vortex wandering on tangential and r.m.s. velocity profiles for different values of the amplitude of the oscillation Δr. (A Burgers vortex model is considered here, and the oscillation is supposed to occur along a straight line perpendicular to the direction along which the mean tangential velocity is estimated.)

tip and decreases towards the foil root. This proves that the spanwise loading of the elliptical foil, which is uniform in an infinite medium, is altered by the confinement: the foil sections are more loaded at tip than at root. In addition, this induced velocity tends to move the tip vortex towards the upper sidewall as shown in figure 14.

The increase in angle of attack is responsible for an increase in lift. This is shown in figure 15 which presents the variation of the measured lift coefficient with the angle of attack for two different values of tip clearance. In its linear part, the lift curve can be characterized by the slope $\partial C_l/\partial\alpha$. Figure 16(*a*) gives the variation of the slope of the lift curve with tip clearance. When the tip clearance is decreased from 60 mm to 0.5 mm, the slope is increased by 30–40%, depending on the Reynolds number. The numerical results obtained from a potential flow computation by Deniset (1996), also presented in figure 16(*a*), corroborate this trend. Note that this NACA 16-020 foil is strongly influenced by Reynolds number, as shown in figure 16(*b*). This has been pointed out by Cerrutti & Pichon (1991).

From the above measurements, it is clear that the confinement wall leads to an

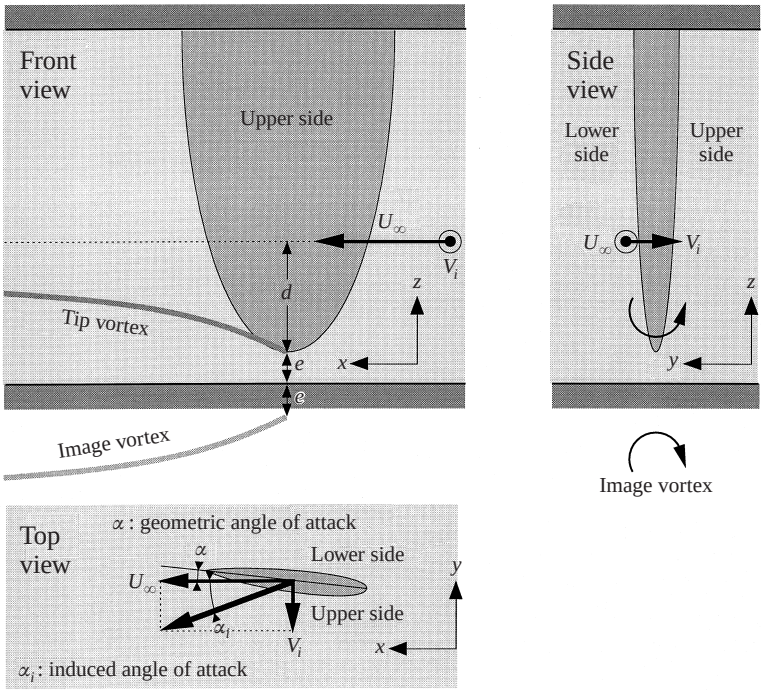

FIGURE 13. Schematic interpretation of the increase in angle of attack due to the confinement.

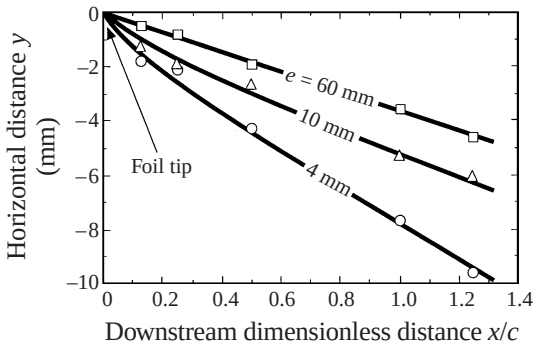

FIGURE 14. Influence of tip clearance on the non-cavitating vortex path in the (x, y)-plane for a flow velocity of $7\,\mathrm{m\,s^{-1}}$ and an angle of attack of $8°$ ($y < 0$ corresponds to the foil upper side).

increase in lift and consequently in vortex strength. It qualitatively explains the premature development of cavitation in confined situations, which is actually shown on the plots of the measured critical cavitation number versus the angle of attack given in figure 5. These data can be replotted versus the lift coefficient (see e.g. Fruman *et al.* 1992). As the lift coefficient increases with confinement, we can expect a collapse of the experimental points.

In comparison with figure 5, figure 17 shows that the experimental data have only a very slight tendency to collapse together; they are far from collapsing along a unique curve. This result suggests that, for different values of tip clearance, the velocity and pressure fields inside the vortex are not similar and do not depend upon a unique parameter, the lift. From LDV measurements, it is clear that the shape of the velocity

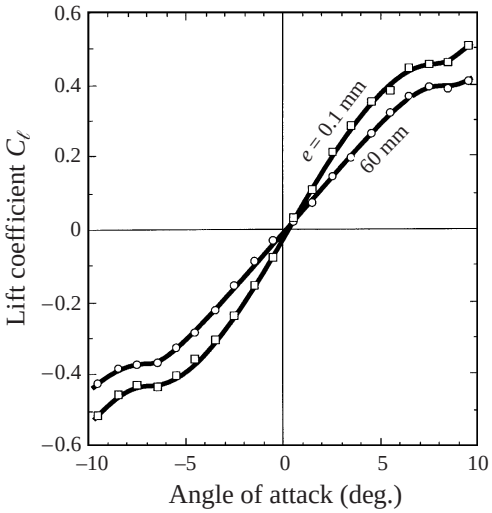

FIGURE 15. Influence of the tip clearance on the variation of the lift coefficient with the angle of attack, for a Reynolds number of 0.84×10^6.

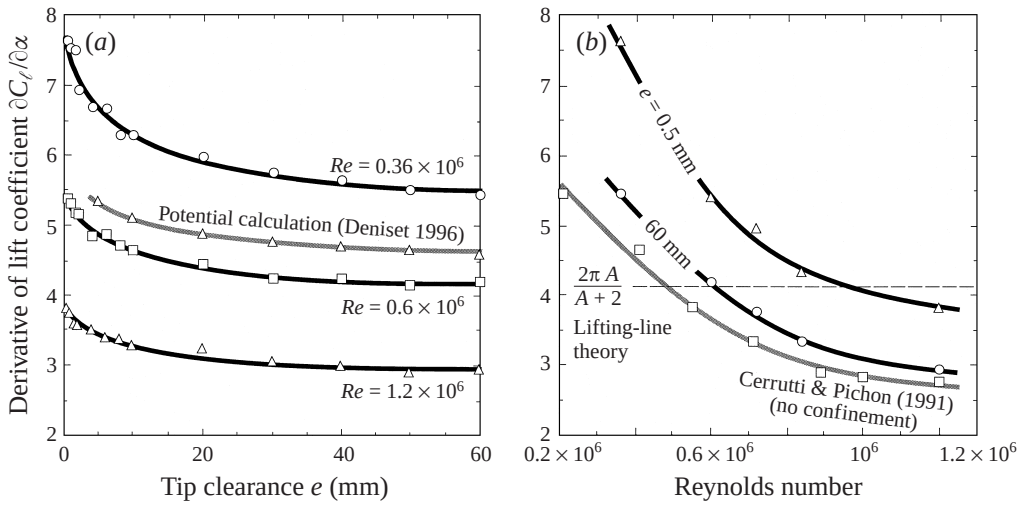

FIGURE 16. Influence of tip clearance and Reynolds number on the derivative of the lift coefficient with the angle of attack.

profiles strongly depends on the degree of confinement. Therefore, it is not surprising that the critical cavitation number is badly correlated with the lift coefficient. The increase in lift does not explain, alone, the lower resistance to cavitation; confinement also induces significant changes in the roll-up mechanism and consequently in the structure of the vortex.

4.3. *Vortex strength in confined situations*

Tip vortex is usually characterized by two parameters: the vortex strength and the size of the vortex viscous core. Consideration of these parameters is based upon the assumption of axisymmetry, which is more especially valid away from the foil and from any confinement wall. The size of the viscous core can be estimated by the

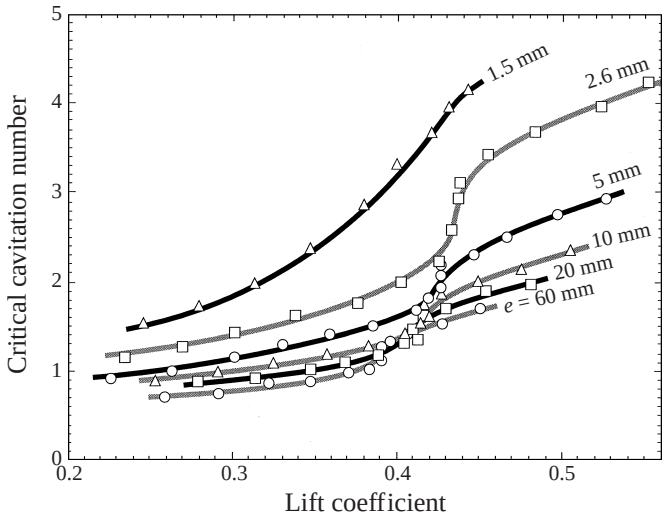

FIGURE 17. Critical cavitation number as a function of the lift coefficient.

distance between the two extrema of velocity. The effect of confinement on the size of the core was already discussed in § 4.1.

The vortex strength is more difficult to quantify under the confined situation. In an infinite medium, the classical procedure consists of computing the product of the measured tangential velocity, V, with the radius, y (see e.g. Fruman *et al.* 1992). If the tip vortex were perfectly axisymmetric, the quantity $2\pi yV$ would measure the circulation along a circle of radius y. In practice, the axisymmetry is far from being valid near the tip foil and the best way to estimate the vortex strength would be to measure the whole velocity field around the tip vortex and to compute the circulation around closed curves. Since velocities have been measured along a line going through the vortex centre, the only possibility for an estimation was to consider the former quantity $2\pi yV$.

Figure 18 presents the profiles of circulation, deduced from LDV measurements, for two different values of tip clearance. We usually consider as a reference the upper side, $y < 0$, which is not affected by the wake of the foil. In the non-confined case, $e = 60$ mm, the circulation exhibits an asymptotic behaviour as the radius increases. In the classical approach, this asymptotic value is considered as a measure of the local vortex strength at the considered downstream location. In confined situations, the profile of circulation does not exhibit such an asymptote, as shown in figure 18. Hence, the classical approach is not applicable to the confined case.

The absence of an asymptote and the tendency of the circulation to decrease at high enough distance from the vortex centre can be qualitatively understood in considering the image vortex. Let us consider the superposition of the influences of two counter-rotating infinite vortices, of constant circulation Γ, at a distance e from both sides of the confinement plate. On an axis parallel to the plate going through the centre of one of the vortices, it can easily be proved that the tangential velocity at a distance y from the vortex centre is given by:

$$V = \frac{\Gamma}{2\pi y} \frac{1}{1 + \left(y/2e\right)^2}. \tag{2}$$

Hence, the circulation $2\pi yV$ vanishes far from the vortex centre. The smaller the tip clearance, the more rapidly the circulation tends to zero. Although this model gives a

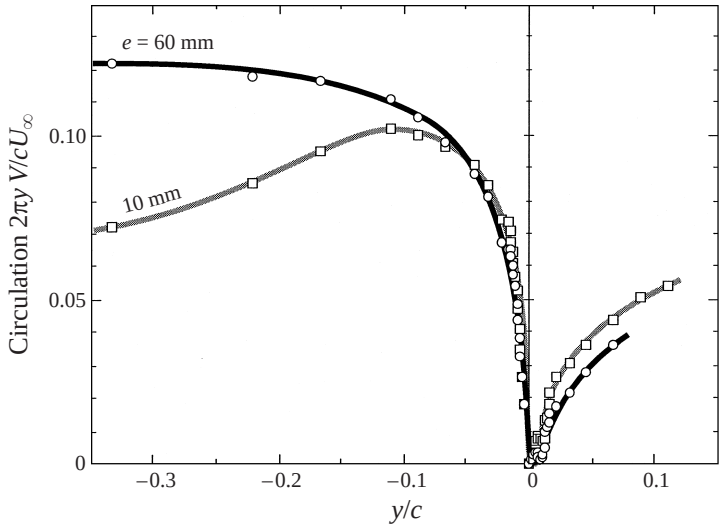

FIGURE 18. Profiles of circulation deduced from the tangential velocity measured by LDV for a flow velocity of $7\,\mathrm{m\,s^{-1}}$, an angle of attack of 8° and at a dimensionless downstream location $x/c = 0.125$. Influence of tip clearance.

satisfactory qualitative behaviour, it is oversimplified, and the dependency on y^{-3} of the flow velocity at high radius is not confirmed experimentally.

As the classical approach based upon the outer potential part of the vortex fails in confined situations, we tried to develop another way of estimating the vortex strength based upon the inner viscous core. In the ideal case of a Rankine vortex of strength Γ and radius a, the circulation is given by $\Gamma = 2\pi a V_{max}$, where V_{max} is the maximum velocity at radius a from the vortex centre. By analogy, we can define the following quantity, which is homogeneous to a circulation:

$$C = \pi D \tfrac{1}{2}(V_{max} + |V_{min}|). \tag{3}$$

In (3), D measures the diameter of the viscous core, estimated by the distance between the two extrema V_{max} and V_{min} of the flow velocity. The consideration of the mean value of both extrema takes into account, to some extent, the strong asymmetry of the velocity profiles. This quantity C is used here as a conventional measure of the vortex strength.

It should be emphasized that this conventional circulation coincides with the usual vortex strength only for a classical Rankine vortex. In the present case, the shape of the tangential velocity profiles, even on the upper side which is the less disturbed one, differs significantly from a Rankine vortex of equal outer strength and equal inner core size, as shown in figure 19. A Burgers model does not fit the experimental data much better. A much better adjustment is usually obtained in the case of measurements between inboard and outboard on a horizontal foil contrary to the present case of measurements between the suction side and the pressure side on a vertical foil (Fruman *et al.* 1992). As the maximum tangential velocity is overestimated by a Rankine model, the so-defined circulation C underestimates the actual vortex strength. This effect is still emphasized by the consideration in (3) of both sides of the velocity profiles, as the maximum velocity on the lower side may be smaller than that on the upper side (see figure 9). Nevertheless, this circulation C is supposed, at

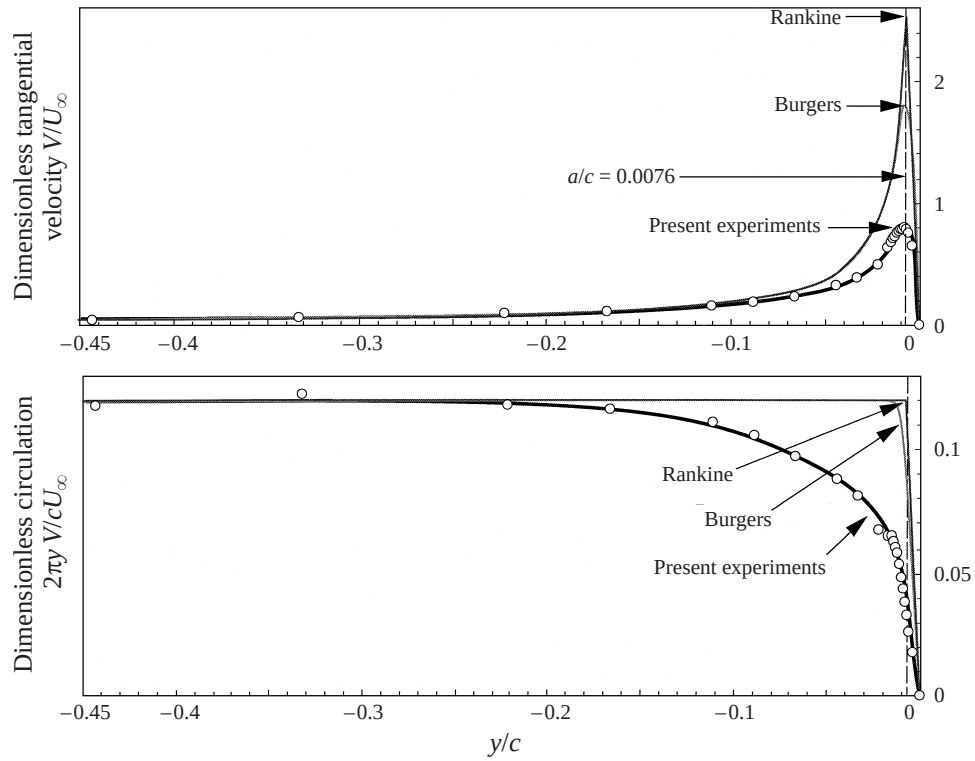

FIGURE 19. Profiles of tangential velocity and circulation for a flow velocity of $7\,\mathrm{m\,s^{-1}}$, an angle of attack of 8° and at a dimensionless downstream location $x/c = 0.125$. Comparison with the Rankine and Burgers models.

best, to be proportional to, and, in any case, to vary like the actual vortex strength. The ratio between both circulations characterizes the shape of the velocity profile.

Figure 20 gives the variation of the so-defined vortex strength with the downstream distance from the foil tip. The influence of confinement is also shown. For a given tip clearance, the vortex strength increases downstream. This trend, which is consistent with the results obtained by other experimenters (e.g. Fruman *et al.* 1995), expresses the roll-up of the vortex sheet emitted by the foil. The confinement does not seem to influence strongly the roll-up mechanism, as present results do not show significant differences in the abscissa at which the plateau of circulation is reached, i.e. the roll-up is completed ($x/c \sim 0.5$).

On the contrary, figure 20 points out a strong influence of tip clearance on the vortex strength. This finding is consistent with present observations on cavitation inception and tends to lend some confidence to the present way of defining the vortex strength.

Table 1 presents a correlation between inception data and vortex strength. The values of the circulation given here correspond to the abscissa $x/c = 0.25$, where the roll-up is not far from being completed as shown in figure 20. Table 1 shows that the incipient cavitation number is approximately proportional to the square of the circulation $\sigma_i \propto C^2$, as we would expect from classical models which assume that the minimum pressure on the vortex axis is proportional to the square of the vortex strength. From Table 1, it is clear that the constant of proportionality depends upon the angle of attack, which tends to prove that the ratio between the actual vortex

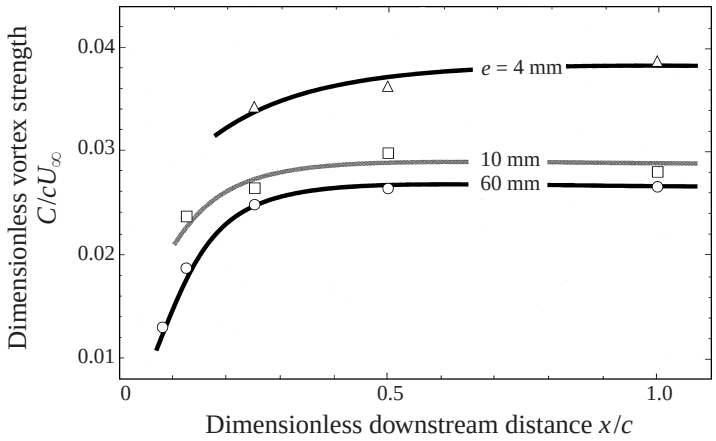

FIGURE 20. Variation of the vortex strength with downstream distance for a flow velocity of 7 m s^{-1} and an angle of attack of 8°. Influence of tip clearance.

α(deg.)	e(mm)	σ_i	C/cU_∞	$\dfrac{\sigma_i}{[C/cU_\infty]^2} \times 10^{-3}$
8	60	1.2	0.0248	2.0
	10	1.6	0.0263	2.3
	4	2.5	0.0342	2.1
5	60	0.74	0.0135	4.1
	10	1.1	0.0166	4.0
	4	1.4	0.0190	3.9

TABLE 1. Comparison of inception data and vortex strength at 7 m s^{-1} and for two different values of the angle of attack 8° and 5° (the circulation C is estimated at station $x/c = 0.25$).

strength and the circulation C defined here also depends upon the angle of attack. Nevertheless, the present results prove that, for a given foil and a given angle of attack, inception data obtained in an infinite medium can be transposed to confined configurations on the basis of LDV measurements of the tangential velocity profiles better than on the basis of measured lift coefficients.

5. Conclusions

Tip vortex cavitation on an elliptical hydrofoil is drastically altered by the presence of a confinement wall in the vicinity of the tip. Confinement induces a large advance in cavitation inception: for a given angle of attack, as tip clearance is reduced, cavitation appears earlier and the critical cavitation number increases.

The non-cavitating structure of the tip vortex is significantly affected by change in the tip clearance. For values of the tip clearance above about 3 mm, the extrema of tangential velocity, measured by LDV, are increased by the confinement. Therefore, the minimum pressure is decreased, which explains the observed trend on critical cavitation numbers.

These trends essentially result from a potential effect. In the present investigation, no viscous effects, connected to the interaction between the tip vortex and the boundary layer which develops on the confinement wall, have been observed to affect

the onset of tip vortex cavitation. The potential effect is qualitatively explained by considering the image vortex, symmetrical to the actual tip vortex with respect to the confinement wall. The velocity it induces leads to an increase in angle at attack, in lift, and consequently in vortex strength. It is the reason why the minimum pressure in the vortex core decreases, and therefore the incipient cavitation number increases.

The classical approach to estimate the local vortex strength, from the asymptote reached outside the core by the momentum of the tangential velocity, appeared not to be valid under confined situations. To overcome this difficulty, a quantity homogeneous to a circulation was defined on the basis of the characteristics of the viscous core, the two extrema of velocity and its diameter. On the few cases available, the incipient cavitation number proved to vary as the square of this circulation. On the contrary, it did not correlate with the measured lift.

For very small values of tip clearance, the large increase in angle of attack induced by the strong confinement can force the flow to stall at the tip. In this case, no more tip vortex cavitation is observed and inception occurs in the form of unsteady small vapour structures, characteristic of a separated flow. LDV measurements show a strong growth in the size of the vortex core, estimated in a direction parallel to the confinement plate, together with a strong decrease of the maximum tangential velocities and therefore corroborate the absence of cavitation in the tip vortex.

This work was conducted with the financial support of Direction des Recherches et de la Technologie (DRET) and is part of the French program Action Concertée Cavitation.

REFERENCES

Arndt, R. E. A., Arakeri, V. H. & Higuchi, H. 1991 Some observations of tip-vortex cavitation. *J. Fluid Mech.* **229**, 269–289.

Arndt, R. E. A. & Keller, A. P. 1991 Water quality effects on cavitation inception in a trailing vortex. *First ASME-JSME Fluids Engineering Conference, Portland, Oregon June 23–27, 1991* (ed. H. Kato & O. Furuya) ASME FED, vol. 116, pp. 1–9.

Belahadji, B., Franc, J. P. & Michel, J. M. 1995 Cavitation in the rotational structures of a turbulent wake. *J. Fluid Mech.* **287**, 383–403.

Billet, M. L. & Holl, W. J. 1979 Scale effects on various types of limited cavitation. In *Intl Symp. on Cavitation Inception, ASME Winter Annual Meeting, New York*, 2–7 December 1979 (ed. W. B. Morgan & B. R. Parkin), pp. 11–23.

Boulon, O. 1996 Etude expérimentale de la cavitation de tourbillon marginal. Effets instationnaires, de germes et de confinement. Thesis (in French), Institut National Polytechnique de Grenoble.

Boulon, O., Franc, J. P. & Michel, J. M. 1997 Tip vortex cavitation on an oscillating hydrofoil. *Trans. ASME* I: *J. Fluids Engng* **119**, 752–758.

Briançon-Marjollet, L. & Merle, L. 1996 Inception, development and noise of a tip vortex cavitation. *21st Symp. on Naval Hydrodyn. Trondheim, Norway.*

Briançon-Marjollet, L. & Michel, J. M. 1990 The hydrodynamic tunnel of I.M.G.: former and recent equipments. *Trans. ASME* I: *J. Fluids Engng* **112**, 338–342.

Cerrutti, P. & Pichon, T. 1991 Cavitation de tourbillon marginal: Effet de la forme en plan. *Report DRET* 91/1035J, Laboratoire d'Hydrodynamique, Ecole Navale, Brest.

Deniset, F. 1996 Modélisation numérique des conditions d'apparition de la cavitation de tourbillon marginal sur une aile-3D. Effet de confinement. Thesis (in French), Institut National Polytechnique de Grenoble.

Dupont, P. & Cerrutti, P. 1992 Comparison between tip vortex development calculations and measurements on an elliptical planform. *3rd European FIDAP Users Group Meeting, Heidelberg, Germany.*

Farrell, K. J. & Billet, M. L. 1994 A correlation of leakage vortex cavitation in axial-flow pumps. *Trans. ASME* I: *J. Fluids Engng* **116**, 551–557.

Franc, J. P. & Michel, J. M. 1985 Attached cavitation and the boundary layer: experimental investigation and numerical treatment. *J. Fluid Mech.* **154**, 63–90.

Fruman, D. H. 1995 The Action Concertée Cavitation research program and accomplishments. *Intl Symp. on Cavitation*, *Deauville*, *France*, pp. 211–217. DCN Bassin d'Essais des Carènes.

Fruman, D. H., Castro, F., Pauchet, A. & Pichon, T. 1994 On tip vortex turbulence, wandering and cavitation occurrence. *2nd Intl Symp. on Cavitation*, *5–7 April 1994*, *Tokyo*, *Japan* (ed. H. Kato), pp. 151–157.

Fruman, D. H., Cerrutti, P., Pichon, T. & Dupont, P. 1995*a* Effect of hydrofoil planform on tip vortex roll-up and cavitation. *Trans. ASME J. Fluids Engng* **117**, 162–169.

Fruman, D. H., Dugué, C. & Cerrutti, P. 1991 Tip vortex roll-up and cavitation. *Cavitation and Multiphase Flow Forum.* ASME FED vol. 109, pp. 43–48.

Fruman, D. H., Dugué, C., Pauchet, A., Cerrutti, P. & Briançon-Marjollet, L. 1992 Tip vortex roll-up and cavitation. *19th Symp. on Naval Hydrodyn. Seoul*, *Korea.*

Fruman, D. H., Pichon, T. & Cerrutti, P. 1995*b* Effect of a drag-reducing polymer solution ejection on tip vortex cavitation. *J. Mar. Sci. Technol.* **1**, 13–23.

Gearhart, W. S. & Ross, J. R. 1991 Tip leakage effects. *1st ASME–JSME Fluids Engineering Conference*, FED vol. 109, pp. 159–164, Portland, USA.

Gowing, S., Briançon-Marjollet, L., Fréchou, D. & Godeffroy, V. 1995 Dissolved gas and nuclei effects on tip vortex cavitation inception and cavitation core size. *Intl Symp. on Cavitation*, *Deauville*, *France*. DCN Bassin d'Essais des Carènes.

Knapp, R. T., Daily, J. W. & Hammitt, F. G. 1970 *Cavitation.* McGraw-Hill.

Laborde, R., Chantrel, P., Retailleau, A., Mory, M. & Boulon, O. 1995 Tip clearance cavitation in an axial flow pump. *Intl Symp. on Cavitation*, *Deauville*, *France*, pp. 173–180.

Lakshminarayana, B. & Horlock, J. H. 1962 Tip-clearance flow and losses for an isolated compressor blade. *Aeronautical Research Council* (*UK*), *Report and Memoranda* 3316.

Le Guen, A., Viot, X., Billard, J. Y. & Fruman, D. H. 1997 Fluctuations des vitesses et biais spatial dans le tourbillon marginal. *Sixièmes Journées de l'Hydrodynamique*, *24–26 Février 1997*, *Nantes*, *France*, pp. 317–328.

McCormick, B. W. 1962 On cavitation produced by a tip vortex trailing from a lifting surface. *J. Basic Engng* **84**, 369–379.

Maines, B. H. & Arndt, R. E. A. 1993 Viscous effects on tip vortex cavitation. ASME FED, vol. 177, pp. 125–132.

Maines, B. H. & Arndt, R. E. A. 1997 Tip vortex formation and cavitation. *Trans. ASME* I: *J. Fluids Engng* **119**, 413–419.

Pauchet, A., Briançon-Marjollet, L., Gowing, S., Cerrutti, P. & Pichon, T. 1994 Effects of foil size and shape on tip vortex cavitation occurrence. *2nd Intl Symp. on Cavitation*, *Tokyo*, *Japan.*

Pauchet, A., Viot, X. & Fruman, D. H. 1996 Effect of upstream turbulence on tip vortex roll-up and cavitation. *Cavitation and Multiphase Flow Forum*, *ASME Fluids Engineering Division Summer Meeting*, *San Diego*, *USA.*

Pichon, T., Fruman, D. H. & Billard, J. Y. 1995 Effect of tripping laminar-to-turbulent boundary layer transition on tip vortex cavitation. *Intl Symp. on Cavitation*, *Deauville*, *France.* DCN Bassin d'Essais des Carènes.

Straka, W. A. & Farrell, K. J. 1992 The effect of spatial wandering on experimental laser velocimeter measurements of the end-wall vortices in an axial flow-pump. *Exps. Fluids* **13**, 163–170.